BULLETIN OF THE POLISH ACADEMY OF SCIENCES
TECHNICAL SCIENCES, Vol. 74(5), 2026, Article number: 1142
DOI: 10.24425/bpasts.2026.1142

Concentric-tube heat exchanger laboratory setup – functional extensions and preliminary tests toward a layered control structure

Krzysztof BARTECKI*

Division of Control Science and Engineering, Opole University of Technology, ul. Prószkowska 76, 45-758 Opole, Poland

Abstract. The paper presents the adaptation and functional extension of a laboratory setup equipped with a concentric-tube heat exchanger for research and educational applications in heat-exchange process control. The introduced hardware and software modifications enable the implementation of a hierarchical, multi-layer control structure representative of industrial heat exchanger systems. As part of the direct control layer, discrete PI controllers were developed to stabilize the key input process variables of the heat exchanger: heating water temperature, heating water flow rate, and heated water flow rate. The controllers were implemented in a real-time *MATLAB/Simulink* environment and experimentally validated on the laboratory setup. The obtained results confirm satisfactory dynamic performance of the control loops and reveal mutual interactions between them. Using the developed control system, steady-state characteristics and temperature distributions of the heat exchanger were experimentally determined. The results confirm both the nonlinear behavior of the process and its distributed-parameter character. Finally, a conceptual design for a supervisory control layer to regulate the outlet temperature of the heated water is proposed. The presented setup constitutes a versatile platform for future experimental studies on hierarchical control structures and advanced control algorithms for heat exchangers.

Keywords: concentric-tube heat exchanger; heat exchanger control; layered control structure; discrete PI control; real-time control; distributed-parameter system.

1. INTRODUCTION

Whether thermal energy is derived from fossil fuels, nuclear power, or renewable sources, its practical utilization necessarily involves heat-exchange processes. Heat exchangers constitute fundamental components of industrial energy and process systems and play a crucial role in power engineering [1], chemical and petrochemical industries [2], as well as heating, ventilation, and air-conditioning (HVAC) systems [3].

From a control engineering perspective, heat exchangers are challenging dynamic systems characterized by nonlinear behavior, multivariable interactions, and sensitivity to operating conditions. These features make them representative benchmark processes for the development and experimental validation of control algorithms, particularly within hierarchical and layered control structures commonly used in industrial automation systems [4, 5].

Among the various types of heat exchangers, concentric-tube (double-pipe) ones are commonly used in laboratory-scale installations, primarily due to their simple geometry and the transparent physical interpretation of heat transfer mechanisms. Although their thermal efficiency is lower than that of more complex industrial exchangers, such as shell-and-tube or plate heat exchangers, concentric-tube configurations are well suited for experimental studies. In particular, they are useful for investigating system dynamics, control loop interactions, and real-time control implementation.

A substantial body of literature addresses the mathematical modeling of heat exchangers, including control-oriented descriptions that capture dominant dynamic effects while maintaining reasonable model complexity [6, 7]. Transfer-function-based models have been used to analyze frequency-domain properties and dynamic behavior of heat exchangers [8, 9]. At the same time, state-space formulations enable systematic controller synthesis and robustness analysis [10, 11]. Such models form the basis for both classical and advanced control strategies.

Alongside modeling efforts, a substantial body of work has addressed the control of heat exchanger systems. Classical PI and PID controllers remain the standard solution in industrial practice, particularly at the direct control layer, where fast stabilization of temperatures and flow rates is required [12, 13]. At higher levels of the control hierarchy, supervisory and cascade control structures are commonly applied to regulate outlet temperatures and compensate for disturbances [14]. More advanced approaches, including adaptive [15], robust [16], H_∞ [17], and model predictive [18] control, have also been reported, offering improved performance under constraints, nonlinearities, and fault conditions [19].

Despite significant theoretical progress, experimental validation of control concepts for heat exchangers remains an important and, in many cases, insufficiently addressed aspect. Much of the reported research is based primarily on simulation studies,

*e-mail: K.Bartecki@po.edu.pl

Manuscript submitted 2026-02-19, revised 2026-04-17, initially accepted for publication 2026-05-12, published in September 2026.

whereas experimental investigations are frequently restricted to single-loop control schemes or static performance characterization. As a result, flexible laboratory platforms that enable the implementation of hierarchical control architectures and the systematic analysis of interactions between control loops remain relatively uncommon.

Motivated by this gap, the present paper addresses the adaptation and enhancement of a laboratory concentric-tube heat exchanger system intended for control-oriented research and education. The introduced hardware and software modifications enable implementation of control algorithms within a layered control structure representative of industrial practice. The direct control layer is examined in detail, with discrete PI controllers developed and experimentally validated to stabilize key input process variables. The developed system can also serve as a suitable platform for future research on supervisory control strategies to regulate outlet temperature in nonlinear, distributed-parameter heat exchanger systems.

2. HEAT EXCHANGER LABORATORY SETUP

Figure 1 presents the laboratory setup developed for experimental investigation of a concentric-tube heat exchanger. The setup, referred to by the manufacturer as TITCA, together with the TIUS base station, the CIB measurement and control module, and a PC equipped with a data acquisition and control card, forms an integrated educational and research platform. It enables experimental studies of steady-state and dynamic heat transfer processes, as well as investigations related to modeling and control of heat exchangers [20].

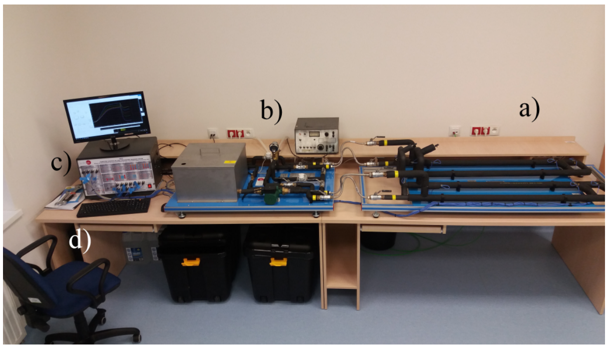

Fig. 1. Concentric-tube heat exchanger laboratory setup

The main components of the laboratory setup, marked in Fig. 1 as a)–d), are described below.

a) The TITCA concentric-tube heat exchanger, with a total length of $L = 4$ m, is designed for experimental investigation of heat transfer between hot (heating) water flowing through the inner tube and cold (heated) water circulating in the annular region between the inner and outer tubes. The setup supports both parallel-flow and counter-flow operation and enables analysis of the influence of the heating and heated water flow rates on transient and steady-state temperature distributions along the exchanger axis.

b) The TIUS base station serves as the central hydraulic and thermal supply unit of the system. It includes a 30 l stainless steel preparatory tank equipped with a 3000 W electric heater, temperature and water level sensors, and a centrifugal pump supplying heating water to the exchanger. The base station also integrates turbine flow meters for measuring the flow rates of heating and heated water, and a pressure reducer to protect the installation against excessive supply pressure, and manual valves to select parallel-flow or counter-flow operation of the exchanger.

c) The CIB measurement and control module acts as an interface between the physical process and the supervisory software. It integrates signals from temperature sensors, flow meters, and actuators, and enables their acquisition and processing in real time. The module also contains a frequency inverter used to control the rotational speed of the heating water circulation pump. Its front panel includes a schematic representation of the installation layout, facilitating operation, monitoring, and diagnostics during experiments.

d) A PC equipped with a National Instruments PCIe-6321 data acquisition and control card serves as the central computational unit of the laboratory system. The card provides multiple analog and digital input/output channels and supports sampling rates up to 250 kS/s, enabling precise acquisition of measurement signals and real-time control of actuators. In combination with SCADA software and the custom *MATLAB/Simulink*-based interface developed by the author, the computer enables data logging, visualization of process variables, and implementation of real-time control algorithms.

The integrated laboratory setup described above allows comprehensive experimental investigation of heat transfer processes. In particular, it enables analysis of the influence of operating conditions and exchanger configurations (parallel-flow and counter-flow) on system dynamics, steady-state characteristics, and control-oriented properties of the heat exchanger.

3. EXTENSIONS OF THE SETUP

3.1. Hardware extension

In the manufacturer's laboratory setup, the heating water flow rate Q_t through the inner tube of the heat exchanger can be adjusted by varying the control voltage u_p. This voltage is applied to the frequency inverter integrated into the CIB module and determines the rotational speed of the heating water circulation pump. Such a configuration enables the realization of a classical heat exchanger control task, namely stabilization of the outlet temperature T_so of the heated water flowing through the outer tube (the exchanger shell) by appropriate adjustment of the heating water flow rate Q_t (see Fig. 2).

Another process variable that significantly influences the outlet temperature T_so of the heated water is the flow rate Q_s of the heated (cold) water supplied by the water distribution system. In practical applications, this flow rate depends on the current demand for heated water and may vary over time, often in a periodic or quasi-periodic manner. From the perspective of the heat exchanger control system, the flow rate Q_s can therefore be

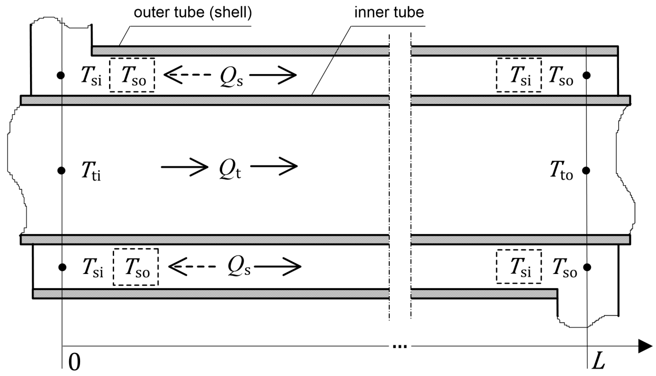

Fig. 2. Simplified diagram of a concentric-tube heat exchanger (dashed lines show counter-flow mode)

treated as a disturbance input affecting the stabilization of the outlet temperature T_{so}.

In the manufacturer-delivered configuration of the laboratory setup, the flow rate Q_s of the heated water can only be adjusted manually by moving a dedicated valve. This limitation significantly restricts experimental studies of automatic control systems for heat exchangers, particularly those focused on disturbance rejection and interactions between control loops.

To overcome this limitation, the original manual valve in the heated water circuit was replaced with a proportional ball solenoid valve. A photograph of the newly installed solenoid valve, together with the previously used manual valve, is shown in Fig. 3.

Fig. 3. Replacement of the manual heated-water valve with a proportional ball solenoid valve

The solenoid valve is driven by an analog control signal generated by the PC-based control system. By using a free analog output channel on the PCIe-6321 data acquisition and control card, the heated water flow rate Q_s can now be automatically adjusted by the control voltage u_v. This hardware extension significantly broadens the range of control scenarios that can be implemented on the laboratory setup. In particular, it enables experimental studies of heat exchanger control systems operating under controlled, time-varying disturbance conditions. Detailed control structures and experimental results enabled by this modification are discussed in the following sections.

3.2. Software extensions

The *Edibon SCADA Software* supplied with the laboratory setup primarily enables real-time monitoring of process variables and hardware states, as well as visualization, fundamental analysis, and reporting of measurement results. However, its functionality for implementing control algorithms is limited. In particular, it does not provide native integration with the *MATLAB/Simulink* environment, which is widely used for rapid prototyping and real-time implementation of control systems.

In contrast, several laboratory installations available at the author's research unit, such as the three-tank system, the magnetic levitation system, or the inverted pendulum on a cart, allow direct integration with *MATLAB/Simulink* [21]. To enable analogous functionality for the heat exchanger setup, the author developed a dedicated software interface that enables real-time communication between the laboratory hardware and the *MATLAB/Simulink* environment.

The software extension is based on the *Simulink Desktop Real-Time* library [22], which enables execution of *Simulink* models in real time on a standard PC running the *Windows* operating system. The library provides access to analog and digital input/output channels of the data acquisition card, configuration of sampling times, and synchronization with the real-time clock. A model constructed using blocks from this library is automatically compiled into executable real-time code and executed by a dedicated real-time kernel.

Figure 4 shows the main *Simulink* diagram developed for real-time operation of the laboratory heat exchanger system. The diagram contains a grouped block representing the physical system of the concentric-tube heat exchanger shown in Fig. 1. The input signals of the heat exchanger block are:

- the control voltage u_p (0–10 V) applied to the frequency inverter of the heating water circulation pump, determining the heating water flow rate Q_t,
- the binary control signal u_h enabling switching the electric heater in the preparatory tank on (1) or off (0),
- the actuator voltage u_v (0–10 V) applied to the proportional solenoid valve controlling the heated water flow rate Q_s.

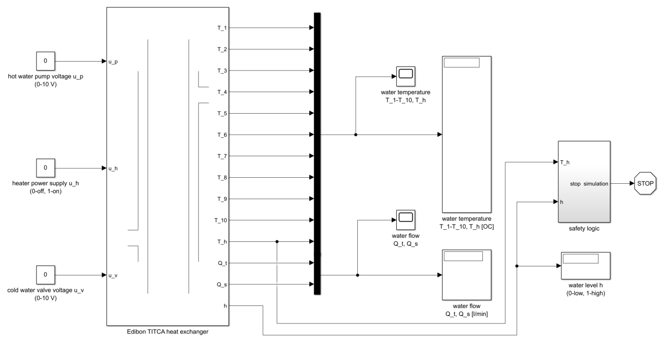

Fig. 4. *Simulink* diagram with the author-developed heat exchanger block used for real-time control experiments

The output signals of the developed heat exchanger block include:

- temperature measurements of the heating water at five locations along the inner tube, T_1–T_5, where $T_1 = T_{ti}$ denotes the inlet temperature and $T_5 = T_{to}$ the outlet temperature of the heating water,

- temperature measurements of the heated water at five locations along the outer tube, T_6–T_{10}, where, depending on the flow configuration, T_6 and T_{10} correspond to the inlet or outlet temperature of the heated water (T_{si} or T_{so}),
- the temperature T_h of the heating water in the preparatory tank,
- the flow rates of the heating and heated water, Q_t and Q_s, respectively,
- a binary signal h indicating the water level in the preparatory tank, where $h = 1$ denotes a sufficient level and $h = 0$ a level below the permissible limit h_{min}.

The internal structure of the heat exchanger block of Fig. 4 is shown in Fig. 5. It includes a subsystem responsible for acquiring measurement signals from temperature, flow, and level sensors, as well as for generating control signals for the actuators. This subsystem was implemented using analog and digital input/output blocks from the *Simulink Desktop Real-Time* library.

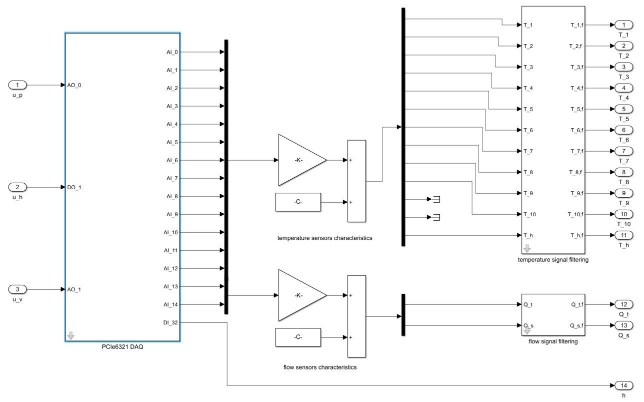

Fig. 5. Internal structure of the heat exchanger block

In turn, Fig. 6 presents the detailed structure of the data acquisition and control subsystem of Fig. 5 based on the PCIe-6321 card. The figure shows the configuration of the analog and digital input/output channels used for interfacing the laboratory hardware with the *MATLAB/Simulink* environment. The channels provide connections to temperature sensors, flow meters, level sensors, the circulation pump, the electric heater, and the proportional solenoid valve.

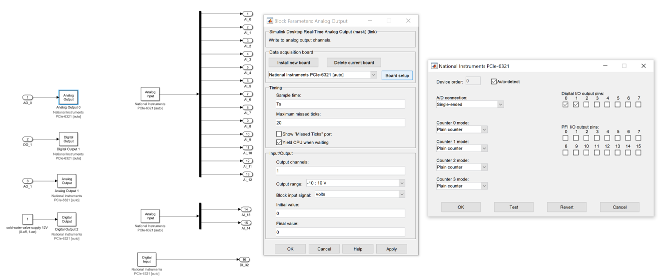

Fig. 6. DAQ subsystem based on the PCIe-6321 card with configured input and output channels

In addition, the subsystem shown in Fig. 5 performs conversion of analog voltage signals (0–10 V) obtained from sensors and measurement transducers into physical quantities. These include temperatures (in degrees Celsius) and flow rates (in liters per minute), calculated according to the calibration characteristics provided by the manufacturer.

To reduce high-frequency measurement noise, low-pass filtering of the acquired signals was implemented within the heat exchanger block using simple infinite-impulse-response (IIR) filters. After preliminary analysis of the recorded signals in both time and frequency domains, a first-order continuous-time low-pass filter with the transfer function

$$G_f(s) = \frac{K}{Ts+1}, \tag{1}$$

and a unit steady-state gain $K = 1$ was adopted as a reference model.

Given the trade-off between noise attenuation and signal delay, the time constant was set to $T = 1$ s for flow rate signals and $T = 5$ s for temperature signals. Assuming a sampling period of $T_s = 0.1$ s and applying the zero-order hold discretization method, the resulting discrete transfer functions are given by

$$G_{Qf}(z) = \frac{0.0952}{z - 0.9048}, \tag{2}$$

for the flow rate signals, and

$$G_{Tf}(z) = \frac{0.0198}{z - 0.9802}, \tag{3}$$

for the temperature signals.

An example illustrating the effectiveness of the applied filtering is shown in Fig. 7. The figure demonstrates that a first-order digital filter provides effective attenuation of high-frequency disturbances while maintaining an acceptable signal delay. Increasing the filter time constant further smooths the signal but introduces a noticeable phase lag, which may adversely affect

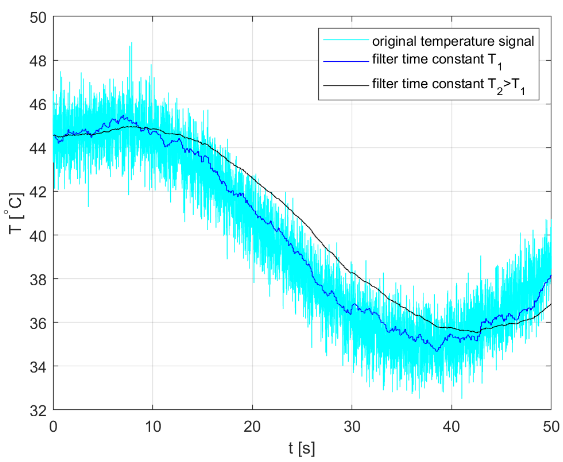

Fig. 7. Temperature signal filtering using discrete low-pass filters with different time constants

the performance and stability of control loops. The selected filter parameters, therefore, represent a compromise between these opposing requirements.

4. HEAT EXCHANGER CONTROL TASKS

4.1. Layered control structure

According to the general layered structure of industrial process control presented in Fig. 8, the lowest layer, referred to as the *process layer* (Layer 0), consists of the controlled object together with the measuring and actuating devices directly connected to it [4, 5].

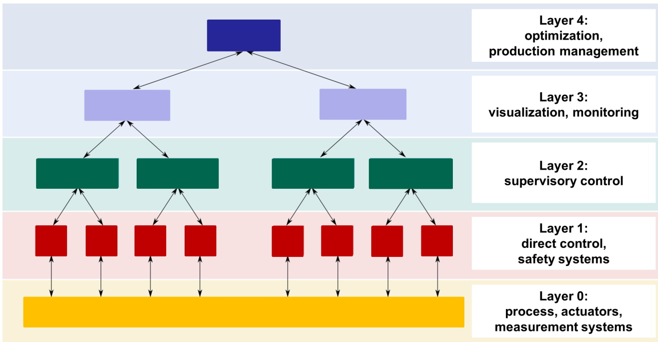

Fig. 8. General hierarchical structure of industrial process control [23]

The next level is the *direct control layer* (Layer 1, DCL). Its task is to regulate fast-changing process variables using sensors, measurement transducers, and actuators in the process layer. Control algorithms implemented at this level are usually relatively simple, such as on–off, proportional (P), proportional–integral (PI), or proportional–integral–derivative (PID) control. These algorithms are typically executed by direct-action controllers, programmable logic controllers, or industrial PCs [24]. In discrete-time implementations, Layer 1 exhibits a high frequency of control interventions, ranging from fractions of a second to several seconds [25].

Layer 2, referred to as the *supervisory control layer*, forms an intermediate level between the DCL and higher-level process supervision and optimization layers. Its primary task is to stabilize the main process variables at their reference values. These reference values may be constant, vary according to a predefined program, or change dynamically in response to external conditions. Setpoint changes can result from operator actions performed at the *visualization and monitoring layer* (Layer 3) or be generated automatically by the *process optimization layer* (Layer 4). Typical examples include temperature scheduling in building heating systems depending on outdoor conditions or time-of-use constraints [14, 26, 27].

Supervisory controllers often operate within cascade control structures, providing reference signals for subordinate controllers located in the DCL. When discrete-time controllers are used, the intervention frequency of Layer 2 is usually several times lower than that of Layer 1. Control algorithms applied at this level may include classical PI or PID controllers as well as more advanced adaptive or predictive strategies. In the present work, the focus is placed on the implementation and experimental verification of tasks associated with the Layer 1 (DCL), including actuator control and safety functions of the heat exchanger system.

4.2. Implementation of the DCL

In the system considered in this study, this layer comprises the heat exchanger, the preparatory hot-water tank, the interconnecting pipelines, and the associated measuring and actuating devices. These include temperature and flow sensors for the heating and heated water, an electric heater installed in the preparatory tank, a circulation pump for the heating water, a proportional solenoid valve for the heated water, and auxiliary manual valves.

Its primary task is to stabilize selected process input variables that are essential for achieving the overall control objectives of the heat exchanger system (see Fig. 4). These variables are:

- the temperature T_h of the heating water in the preparatory tank,
- the flow rate Q_t of the heating water supplied to the exchanger,
- the flow rate Q_s of the heated water flowing through the exchanger.

The above control objectives are realized by manipulating the input signals of the corresponding actuators, namely:

- the electric power supplied to the heater in the preparatory tank, controlled by a binary signal $u_h \in \{0, 1\}$,
- the supply voltage u_p of the circulation pump inverter, with $0 \le u_p \le 10$ V,
- the control voltage u_v of the proportional solenoid valve for the heated water, with $0 \le u_v \le 10$ V.

Three discrete-time controllers execute the direct control tasks listed above, further referred to as:

- Heater Discrete Controller (HDC),
- Pump Discrete Controller (PDC),
- Valve Discrete Controller (VDC).

In addition to regulation tasks, the DCL also includes elements responsible for process protection (see Fig. 8). These comprise:

- a differential pressure controller integrated by the manufacturer into the TIUS base station, protecting the installation against excessive pressure in the water supply network,
- a safety logic system implemented in the *MATLAB/Simulink* environment (see Fig. 4), which stops the operation of the setup by:
  - switching off the heater,
  - stopping the circulation pump,
  - closing the heated-water valve,

  when the maximum permissible water temperature $T_{h,max}$ in the preparatory tank is exceeded or when its level falls below the allowable limit h_{min}.

To accomplish the three direct control tasks, discrete proportional–integral (PI) controllers were implemented using standard *MATLAB/Simulink* library blocks. The controllers operate in a positional form and are described by the following discrete transfer function:

$$G_c(z) = \frac{U_n(z)}{E_n(z)} = K_p \left(1 + \frac{T_s}{T_i} \frac{z}{z-1}\right), \tag{4}$$

where K_p denotes the proportional gain, T_i is the integral time constant, and T_s is the sampling period.

In equation (4), $E_n(z)$ denotes the Z-transform of the normalized discrete control error $e_n[k]$, whose value is confined to the interval $[-1, 1]$. The discrete error signal is defined as

$$e[k] = y_{\text{ref}}[k] - y[k] \tag{5}$$

where $k = 0, 1, 2, \ldots$ denotes the discrete-time index corresponding to the sampling instants $t_k = kT_s$. The signals $y_{\text{ref}}[k]$ and $y[k]$ represent the reference (setpoint) and the measured output, respectively. The normalization of the error signal is performed to ensure scale invariance, improve numerical properties, and facilitate controller tuning, according to

$$e_n[k] = 2\frac{e[k] - e_{\min}}{e_{\max} - e_{\min}} - 1, \tag{6}$$

with the boundary values $e_{\min}$ and $e_{\max}$ selected individually for each control loop, depending on the admissible range of the corresponding controlled variable.

In turn, $U_n(z)$ in equation (4) denotes the Z-transform of the normalized control signal $u_n[k]$, obtained at the controller output and satisfying $u_n[k] \in [-1, 1]$. It is subsequently converted into the physical control signal applied to the actuator according to

$$u[k] = \frac{u_n[k](u_{\max} - u_{\min}) + u_{\max} + u_{\min}}{2}, \tag{7}$$

where $u_{\min}$ and $u_{\max}$ denote the minimum and maximum admissible actuator input values.

The controller parameters in equation (4) were determined using the second Ziegler–Nichols tuning method [28, 29]. This method assumes that the step response of a wide class of asymptotically stable processes can be approximated by the response of a first-order system with time delay [30]:

$$G_m(s) = \frac{K\,e^{-T_d s}}{Ts + 1}, \tag{8}$$

where K denotes the steady-state gain, T is the time constant, and T_d represents the transport delay.

The tuning procedure consists of an identification experiment in which the step response of the controlled process is recorded and the parameters K, T, and T_d of the model given by equation (8) are estimated. Based on these parameters, the settings for P, PI, or PID controllers are determined using empirical formulas proposed by Ziegler and Nichols. The resulting tuning represents a compromise between fast transient response and a sufficient stability margin. The method is particularly suitable for disturbance rejection tasks, for which moderate overshoot is acceptable.

In the present study, the tuning procedure was applied independently to the three subsystems associated with the respective actuators: the heating water circulation pump, the electric heater in the preparatory tank, and the proportional solenoid valve of the heated water. The obtained PI controller settings are summarized in Table 1. Since the controllers are implemented in discrete time, the sampling period T_s is additionally specified. For flow rate control loops, a sampling period of $T_s = 0.1$ s was adopted, whereas for temperature control, $T_s = 0.5$ s was found sufficient. These values are consistent with typical sampling times used in industrial control applications [24].

Table 1
Parameter settings for the DCL controllers

Controller	Signal limits				Settings		
	$e_{\min}$	$e_{\max}$	$u_{\min}$	$u_{\max}$	T_s	K_p	T_i
PDC	−2.7	2.7	0	10	0.1 s	0.8	1.5 s
HDC	−50	50	−1	1	0.5 s	15	100 s
VDC	−3.5	3.5	0	3	0.1 s	0.6	8 s

To prevent integrator windup, which occurs when the control signal saturates while the integral term continues to accumulate, an anti-windup mechanism based on the clamping method was applied. In this approach, the integration of the error signal is suspended whenever the controller output reaches one of its saturation limits, and resumed once the output returns to the admissible range [31, 32].

Figure 9 presents the internal structure of the PDC developed in this work, including the grouped controller block and its parameter configuration dialog. The structures of the HDC and VDC blocks are analogous and differ only in parameter values listed in Table 1.

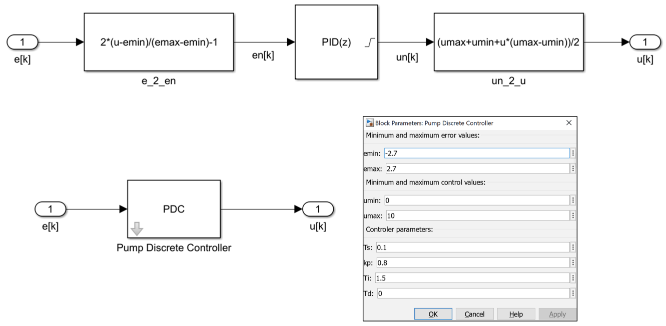

Fig. 9. Structure of the PDC block with the parameter configuration dialog

In the case of the HDC system, the actuator operates in a binary on–off mode. Therefore, a pulse-width modulation (PWM) block was placed downstream of the controller. It converts the continuous-valued control signal generated by the PI controller into a binary signal with an appropriate duty cycle, enabling quasi-continuous control of the heating power [33].

Using the considered controller blocks together with the *Simulink* subsystems described in Section 3.2, which represent the heat exchanger system, safety logic, and auxiliary signal processing elements, the complete real-time control diagram shown in Fig. 10 was constructed. This diagram represents the direct control and safety layer (Layer 1), while the physical heat exchanger system constitutes the process layer (Layer 0). Based on

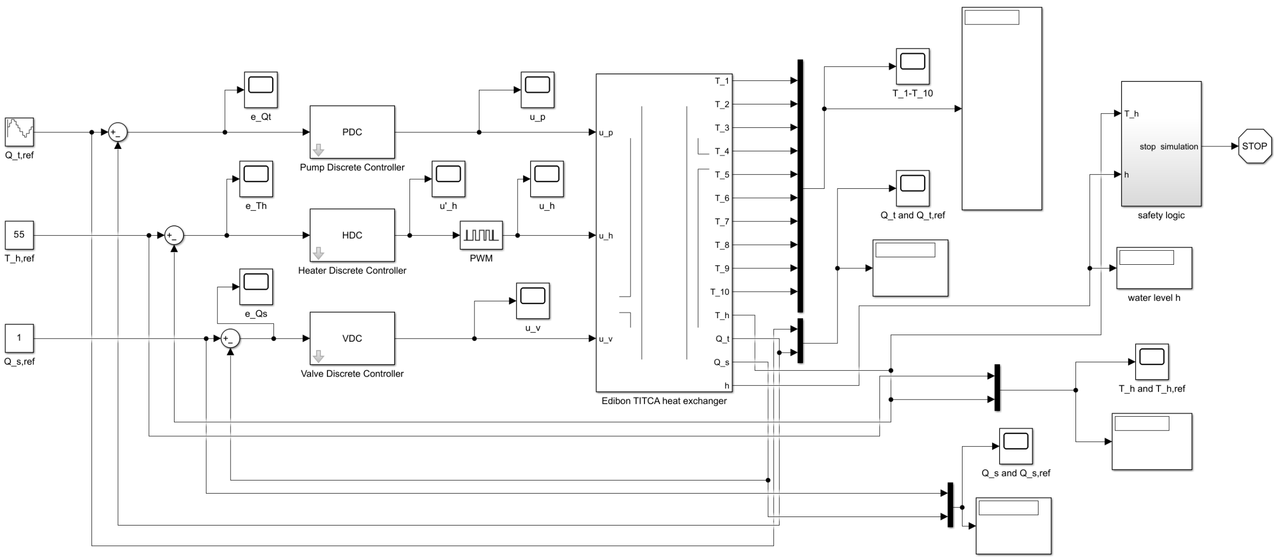

Fig. 10. *Simulink* diagram for testing controllers and safety logic forming the DCL of the laboratory heat exchanger system

this configuration, experimental investigations of the individual direct control subsystems were conducted, and selected results are presented in the following section.

5. PRELIMINARY EXPERIMENTAL RESULTS

The experimental studies were carried out according to typical scenarios encountered in control tasks for heat exchanger systems. In particular, attention was focused on the nature of changes in the reference values of the main input process variables controlled by the DCL.

The role of the PDC was to control the heating water flow rate Q_t according to a predefined program, ensuring tracking of the instantaneous reference value $Q_{t,ref}$. In the target hierarchical control structure, this reference value will be generated by a supervisory controller that regulates the outlet temperature T_{so} of the heated water.

The HDC was tasked with stabilizing the temperature T_h of the water in the preparatory tank at a constant reference value $T_{h,ref}$, despite disturbances arising mainly from variations in the heating water flow rate Q_t enforced by the PDC.

In turn, the VDC was used to stabilize the flow rate Q_s of the heated water at a constant reference value $Q_{s,ref}$. In practical applications, the system operator may adjust this value to reflect current demand for thermal energy.

As described above, the individual control loops interact with one another. A variable regulated in one loop simultaneously acts as a disturbance in another. For example, an increase in the reference value $Q_{t,ref}$ causes the PDC to increase the rotational speed of the circulation pump, leading to a higher heating water flow rate Q_t. This, in turn, results in a decrease in the water temperature T_h in the preparatory tank, which constitutes a disturbance to the HDC-controlled subsystem. The HDC compensates for this effect by increasing the heating power supplied to the tank.

5.1. Preparatory tank water temperature control

The first stage of system operation after start-up was the heating of the water in the preparatory tank to the reference temperature $T_{h,ref}$. During this phase, the heat exchanger itself was inactive, which means that both flow rates were set to zero ($Q_{t,ref} = Q_{s,ref} = 0$ l/min). The initial temperature of the water in the tank was equal to the ambient temperature.

The reference temperature of the preparatory tank was set to $T_{h,ref} = 55°C$. The main performance requirement for the controller was a regulation time of no more than 1 h and an overshoot not exceeding 5%, defined with respect to the steady-state value.

Figure 11 shows the time evolution of the water temperature T_h in the preparatory tank during a 5400 s experiment, while Fig. 12 presents the corresponding control signals generated by the HDC. The signal u'_h denotes the controller output, whereas u_h represents its binary PWM-converted form applied to the electric heater.

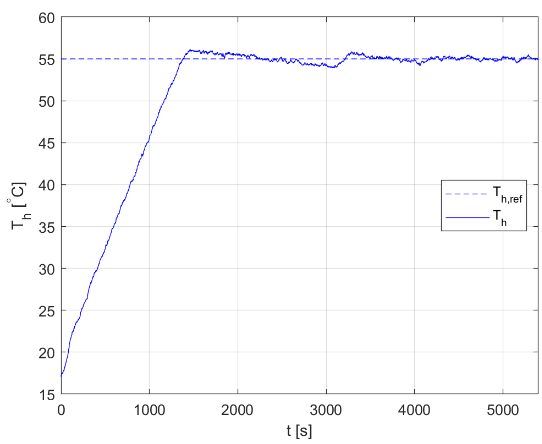

Fig. 11. Response of the constant temperature control system of the preparatory water tank

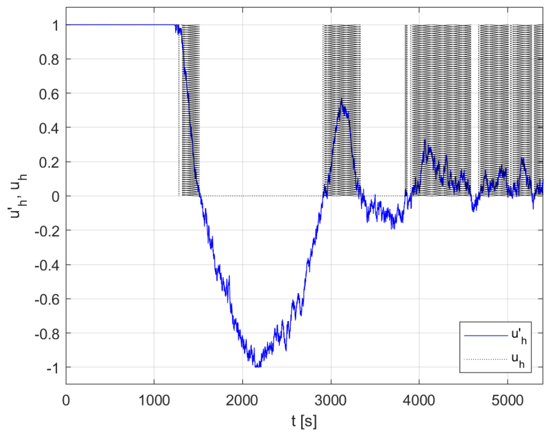

Fig. 12. Control signal profiles in the constant temperature control system of the preparatory water tank

The obtained results confirm that the control objective was achieved. Both the regulation time and the overshoot, manifested as small oscillations around the reference value, remained within the assumed limits.

5.2. Heat exchanger operation with programmed flow control

After the water in the preparatory tank reached the desired temperature, the heat exchanger was put into operation by activating the heating water circulation pump and opening the heated water valve. The heat exchanger operated in a counter-flow configuration.

During a 12 000 s experiment, the reference value of the heating water flow rate $Q_{\mathrm{t,ref}}$ was changed every 1200 s according to a predefined schedule. In contrast, the reference value of the heated water flow rate was kept at the constant nominal value $Q_{\mathrm{s,ref}} = Q_{\mathrm{s,n}} = 1$ l/min. The main performance requirement for the PDC was a regulation time of 30 s or less, with an allowable overshoot below 10%, defined with respect to the steady-state value.

Figure 13 presents the measured flow rates of the heating and heated water, while Fig. 14 shows the corresponding control signals generated by the PDC, VDC, and HDC. For clarity, the binary heater control signal u_{h} is omitted.

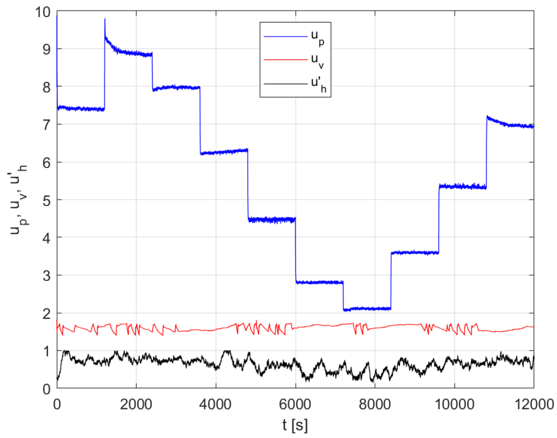

Fig. 14. Control signal profiles in the programmed control system of the heating water flow rate Q_{t}

The PDC accurately tracks the programmed reference values of $Q_{\mathrm{t,ref}}$ while satisfying the assumed transient performance requirements. In the VDC-controlled loop, noticeable short-term fluctuations in the flow rate Q_{s} are observed, most likely due to variations in the supply water pressure. Nevertheless, the flow rate remains satisfactorily stabilized around the nominal value.

To enable a quantitative assessment of the performance of the considered control loops, the following discrete-time approximations of integral performance indices are used [34]:

$$\mathrm{IAE} = T_{\mathrm{s}} \sum_{k=0}^{N} |e[k]| \tag{9}$$

and

$$\mathrm{ITAE} = T_{\mathrm{s}} \sum_{k=0}^{N} k\, T_{\mathrm{s}}\, |e[k]|, \tag{10}$$

where N denotes the number of samples corresponding to the final time instant $T_{\mathrm{f}} = 12\,000$ s, i.e., $N = T_{\mathrm{f}}/T_{\mathrm{s}}$.

For illustration, the values of the indices (9) and (10), obtained for the PDC system with nominal controller parameters given in Table 1, are summarized in Table 2.

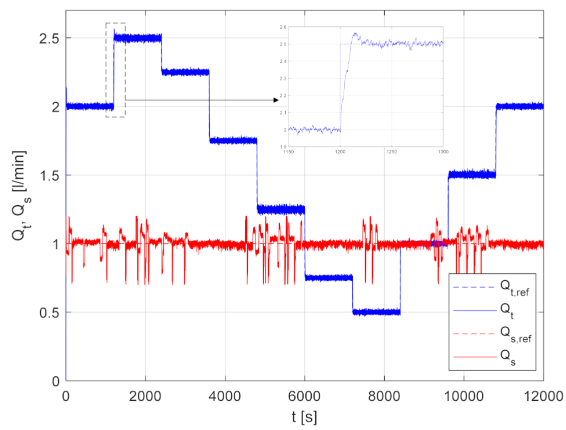

Fig. 13. Response of the programmed control system of the heating water flow rate Q_{t}

Table 2
Performance indices for different PDC settings

Controller settings		Performance indices	
K_{p}	T_{i}	IAE	ITAE
0.8 (nom.)	1.5 s (nom.)	106.5	$6.18 \cdot 10^5$
0.4 (−50%)	1.5 s (nom.)	109.7	$6.35 \cdot 10^5$
1.2 (+50%)	1.5 s (nom.)	107.1	$6.21 \cdot 10^5$
0.8 (nom.)	0.75 s (−50%)	108.4	$6.29 \cdot 10^5$
0.8 (nom.)	2.25 s (+50%)	107.5	$6.22 \cdot 10^5$

To assess the robustness of the considered control loop, a detuning study was performed by varying both controller parameters around their nominal values. The results indicate that the PDC system remained stable even under ±50% variations in the K_p and T_i parameters. However, these changes led to a deterioration in control performance, as quantified by the IAE and ITAE indices shown in Table 2. A similar analysis of the two remaining control loops yielded qualitatively similar results to those presented above.

Figure 15 shows the temperature profiles measured along the heat exchanger during the discussed control experiment. It follows that the HDC effectively stabilizes the preparatory tank water temperature at $T_{h,ref} = 55°C$ despite the varying thermal load imposed by changes in Q_t.

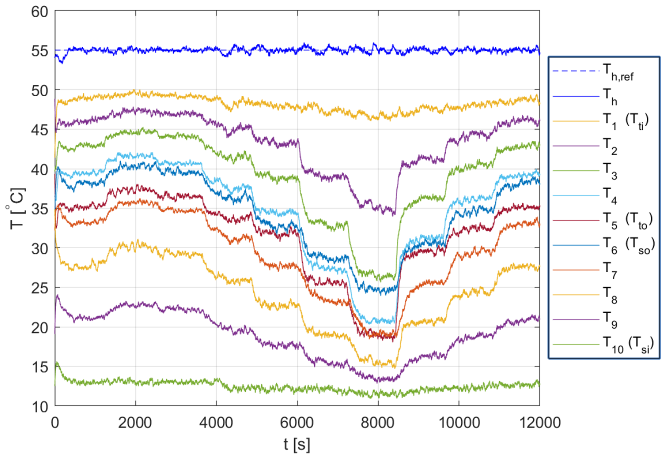

Fig. 15. Temperature profiles of the heating water T_t and the heated water T_s in the heat exchanger

Due to the counter-flow configuration, the temperature T_{10} corresponds to the inlet temperature T_{si} of the heated water, whereas T_6 represents its outlet temperature T_{so}. The latter constitutes the primary controlled variable in the planned supervisory control layer.

5.3. Steady-state characteristics and temperature profiles

Additional similar experiments were performed for other values of the heated-water flow rate ($Q_{s,ref} = 2$ l/min and $Q_{s,ref} = 3$ l/min), as well as for the parallel-flow configuration. Based on all experiments conducted, approximate steady-state characteristics and corresponding temperature distributions were determined and are presented in Figs. 16–18.

Figure 16 presents the approximate steady-state (static) characteristics $T_{so} = f(Q_t)$ obtained for both parallel-flow and counter-flow configurations of the heat exchanger and for several values of the heated water flow rate Q_s. The plots clearly demonstrate the nonlinear nature of the process. For low values of the heating water flow rate Q_t, relatively small changes in the control input result in pronounced variations of the outlet temperature T_{so}, whereas for higher flow rates the sensitivity of the output temperature decreases significantly.

This behavior is a direct consequence of the bilinear structure of the heat exchanger model equations, which include products

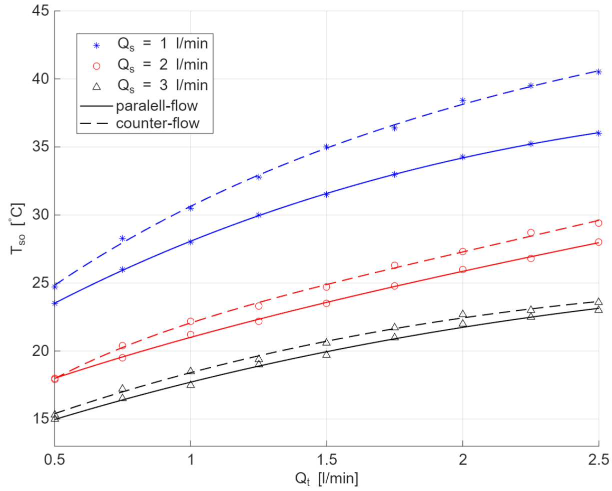

Fig. 16. Experimental steady-state characteristics $T_{so} = f(Q_t)$ of the heat exchanger for different Q_s

of flow rates and temperatures, in particular the product of the heating water flow rate Q_t and the heated water temperature T_s [35]. The results also confirm the well-known superiority of the counter-flow configuration, which yields a higher outlet temperature T_{so} for the same value of Q_t compared to the parallel-flow arrangement.

Figures 17 and 18 show the approximate steady-state temperature profiles $T_t(l)$ and $T_s(l)$ of the heating and heated fluids measured along the exchanger axis for the parallel-flow and counter-flow configurations, respectively. The temperature distributions reveal significant spatial variations along the length of the exchanger, which depend on the operating conditions and flow configuration.

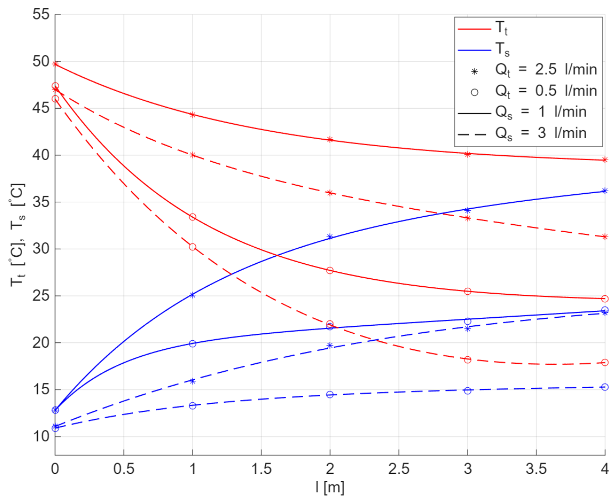

Fig. 17. Experimental steady-state temperature distributions $T_t(l)$ and $T_s(l)$ for the parallel flow with different Q_t and Q_s

The presented results confirm that the analyzed heat exchanger exhibits distributed-parameter (i.e., spatio-temporal) characteristics. This implies that temperature variations occur both temporally and spatially within the heat exchanger. Moreover, the characteristics obtained here confirm that the counter-

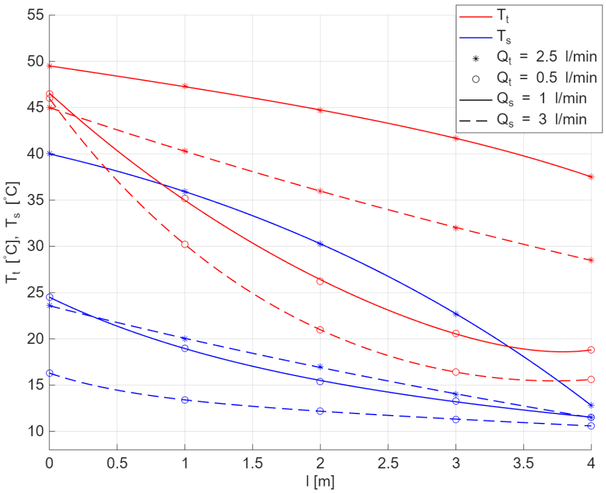

Fig. 18. Experimental steady-state temperature distributions $T_t(l)$ and $T_s(l)$ for the counter flow with different Q_t and Q_s

flow configuration provides a more uniform temperature difference between the heating and heated fluids along the exchanger length. This promotes efficient and stable heat transfer and reduces thermal stresses in the exchanger structure (see Figs. 17 and 18). Additionally, it should be emphasized that the characteristics obtained here are consistent with those previously derived using analytical methods, based on the heat exchanger equations applicable under steady-state conditions [8, 36].

In summary, the experimental results obtained for all three direct control loops forming the DCL demonstrate that the adopted discrete PI controllers successfully achieve their respective control objectives. At the same time, the experiments confirm the heat exchanger's nonlinear, distributed-parameter nature, which justifies the need for an advanced hierarchical control structure and motivates the introduction of a supervisory control layer discussed in the following section.

6. CONCEPTUAL DESIGN FOR SUPERVISORY CONTROL

The discussion and experimental results presented in the preceding chapters concerned the two lowest layers of the hierarchical control structure shown in Fig. 8, namely the process layer (Layer 0) and the direct control layer (Layer 1). It was demonstrated that the controllers operating within the Layer 1 effectively stabilize the selected input process variables of the heat exchanger system. Following a bottom-up development strategy, the next step is the conceptual design of the supervisory control layer (Layer 2).

A detailed structure of the hierarchical control system proposed for the heat exchanger is shown in Fig. 19. In addition to the previously discussed layers, the structure includes a supervisory controller, denoted as OTC (Outflow Temperature Controller). Its primary task is to stabilize the outlet temperature T_{so} of the heated water at the desired reference value $T_{so,ref}$.

The reference value $T_{so,ref}$ may be constant or may vary according to a predefined program, for example as a result of the operation of a higher-level process optimization layer. In the latter case, the supervisory control system performs the so-called programmed control.

In the simplest configuration, the OTC controller may operate in an open-loop (feed-forward) mode. In such a case, the controller determines the reference value of the heating water flow rate $Q_{t,ref}$ for the subordinate Pump Discrete Controller (PDC) based on the desired outlet temperature $T_{so,ref}$ and, optionally, on the known reference value of the heated water flow rate $Q_{s,ref}$. This approach may rely, for example, on the steady-state relationship $T_{so} = f(Q_t)$ obtained experimentally in Section 5 (see Fig. 16). Knowledge of the disturbance signal Q_s enables partial compensation of its influence on the outlet temperature in advance.

In a more typical configuration, feedback information is provided by temperature sensors measuring the outlet temperature T_{so} of the heated water. This allows the implementation of

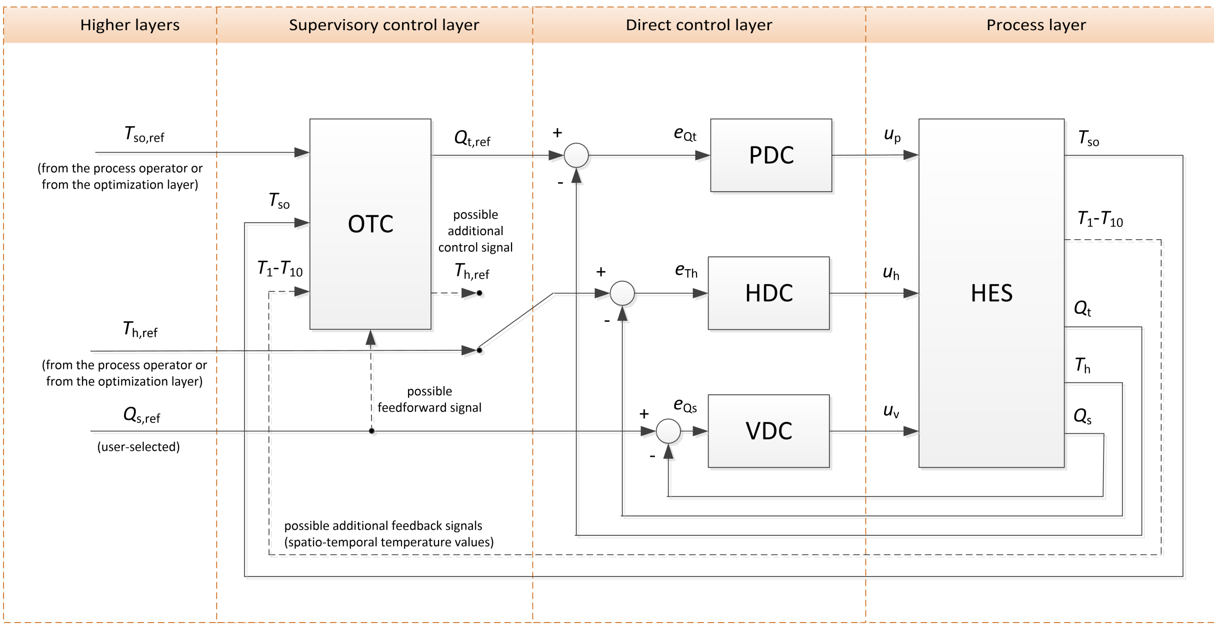

Fig. 19. Concept of a layered control structure for the heat exchanger system (HES)

a closed-loop supervisory control system, in which the OTC controller operates based on the control error defined as

$$e_{\mathrm{so}} = T_{\mathrm{so,ref}} - T_{\mathrm{so}}\,. \tag{11}$$

In this structure, OTC and PDC constitute a cascade control system, where OTC provides the reference signal $Q_{\mathrm{t,ref}}$ to PDC operating in DCL.

From a technological perspective, the heating water flow rate Q_{t} constitutes the most convenient manipulated variable for regulating the outlet temperature T_{so}. The PDC performs its stabilization within the DCL. An alternative way to influence the outlet temperature is to vary the heating water inlet temperature T_{ti} supplied from the preparatory tank. This variable is indirectly controlled by the HDC, which stabilizes the temperature T_{h} of the heating water in the tank.

However, the dynamic properties of the corresponding control loops differ significantly. While the regulation time of the Q_{t} control loop typically ranges from a few to several tens of seconds (see results in Fig. 13), the temperature control loop associated with T_{h} exhibits much slower dynamics, with regulation times reaching several hundred or even several thousand seconds (see Fig. 11). Consequently, variations of T_{h} do not allow compensation of high-frequency disturbances, but may be effectively used for long-term adjustments, such as night-time or weekend temperature scheduling. In such cases, the reference value $T_{\mathrm{h,ref}}$ could be generated by a higher-level optimization layer and supplied to the subordinate HDC.

Regarding the control algorithms employed at the supervisory level, both classical and advanced approaches can be considered. These include PI or PID controllers, as well as adaptive, predictive, or data-driven methods [15, 18, 37]. For complex plants characterized by nonlinearity, parameter variability, or spatio-temporal dynamics, advanced control strategies may offer improved performance. However, their effectiveness strongly depends on the modeling approach adopted during controller synthesis.

In the case of heat exchangers, which are distributed parameter systems, a commonly used approach is the so-called early lumping. In this strategy, an approximated lumped-parameter model is first derived from the original distributed model, and controller synthesis is subsequently performed using classical methods developed for lumped-parameter (finite-dimensional) systems [38, 39].

An alternative approach, referred to as late lumping, involves directly synthesizing the controller based on the plant's distributed-parameter model, typically formulated as a system of partial differential equations [40, 41]. The resulting controller also exhibits distributed-parameter characteristics and must be discretized for practical implementation. Although this approach entails significantly higher computational complexity, it may potentially lead to improved control performance.

The extended experimental setup presented in this paper provides a suitable platform for investigating both early and late lumping strategies. Future work will focus on simulation-based and experimental studies to evaluate the benefits and limitations of these approaches when applied to the supervisory control of heat exchanger systems.

7. SUMMARY

The paper presented the adaptation and functional extension of a laboratory concentric-tube heat exchanger. The introduced hardware and software modifications significantly extended its original capabilities. They enable the implementation of a hierarchical, multi-layer control structure representative of industrial heat-exchange systems.

As part of the DCL, discrete PI controllers were developed and experimentally validated to stabilize the key input process variables of the heat exchanger: heating water temperature, heating water flow rate, and heated water flow rate. Experimental investigations confirmed that the adopted control solutions ensure satisfactory dynamic performance and robustness against mutual interactions among individual control loops. The results also clearly demonstrated the heat exchanger's nonlinear behavior and distributed-parameter nature, as evidenced by its steady-state characteristics and spatial temperature profiles, respectively.

In addition to validating this layer, the paper proposed a conceptual design for a supervisory control layer to regulate the outlet temperature of the heated water. The discussion addressed possible control structures, manipulated variables, and modeling strategies, including both early and late lumping approaches. The presented laboratory setup offers a suitable platform for future experimental studies on supervisory control algorithms, ranging from classical cascade control to advanced adaptive and predictive methods.

Overall, the developed laboratory system constitutes a versatile research and educational platform. It enables experimental verification of control-oriented heat exchanger models, investigation of multi-layer control architectures, and practical assessment of control algorithms for systems with spatio-temporal dynamics. The setup can also support student projects and doctoral research in the modeling, identification, and control of heat-exchange processes.

REFERENCES

[1] D.S. Patil, R.R. Arakerimath, and P.V. Walke, "Thermoelectric materials and heat exchangers for power generation – a review," *Renew. Sustain. Energy Rev.*, vol. 95, pp. 1–22, 2018, doi: 10.1016/j.rser.2018.07.003.

[2] O.B. Doldán, M.J. Bagajewicz, and J. Cerdá, "Designing heat exchanger networks for existing chemical plants," *Comput. Chem. Eng.*, vol. 9, no. 5, pp. 483–498, 1985, doi: 10.1016/0098-1354(85)80024-7.

[3] W. Radziszewska, M.A. Bugaj, M. Łuniewski, G. Hoogsteen, P. Chaja, and S. Bykuć, "Testing of a price-based system for power balancing on real-life HVAC installation in real life," *Bull. Pol. Acad. Sci. Tech. Sci.*, vol. 70, no. 2, p. e140690, 2022.

[4] S. Skogestad, "Control structure design for complete chemical plants," *Comput. Chem. Eng.*, vol. 28, no. 1, pp. 219–234, 2004, doi: 10.1016/j.compchemeng.2003.08.002.

[5] P. Tatjewski, *Advanced Control of Industrial Processes: Structures and Algorithms*, ser. Advances in Industrial Control. London, United Kingdom: Springer, 2007.

[6] R. Prasad, "Generalized solution and effectiveness for concentric tube heat exchangers," *Int. J. Heat Mass Transf.*, vol. 31, no. 12, pp. 2571–2578, 1988, doi: 10.1016/0017-9310(88)90183-4.

[7] A. Zavala-Río and R. Santiesteban-Cos, "Reliable compartmental models for double-pipe heat exchangers: An analytical study," *Appl. Math. Model.*, vol. 31, no. 9, pp. 1739–1752, 2007, doi: 10.1016/j.apm.2006.06.005.

[8] K. Bartecki, "Transfer function-based analysis of the frequency-domain properties of a double pipe heat exchanger," *Heat Mass Transf.*, vol. 51, no. 2, pp. 277–287, 2015, doi: 10.1007/s00231-014-1410-5.

[9] W. Al Hadad, D. Maillet, and Y. Jannot, "Modeling unsteady diffusive and advective heat transfer for linear dynamical systems: A transfer function approach," *Int. J. Heat Mass Transf.*, vol. 115, pp. 304–313, 2017, doi: 10.1016/j.ijheatmasstransfer.2017.07.009.

[10] Y. Wang, S. You, W. Zheng, H. Zhang, X. Zheng, and Q. Miao, "State space model and robust control of plate heat exchanger for dynamic performance improvement," *Appl. Therm. Eng.*, vol. 128, pp. 1588–1604, 2018, doi: 10.1016/j.applthermaleng.2017.09.120.

[11] K. Bartecki, "Approximate state-space and transfer function models for 2×2 linear hyperbolic systems with collocated boundary inputs," *Int. J. Appl. Math. Comput. Sci.*, vol. 30, no. 3, pp. 475–491, 2020, doi: 10.34768/amcs-2020-0035.

[12] P. Laszczyk, "Simplified modeling of liquid-liquid heat exchangers for use in control systems," *Appl. Therm. Eng.*, vol. 119, pp. 140–155, 2017, doi: 10.1016/j.applthermaleng. 2017.03.033.

[13] A. Vasičkaninová, M. Bakošová, L. Čirka, M. Kalúz, and J. Oravec, "Robust controller design for a laboratory heat exchanger," *Appl. Therm. Eng.*, vol. 128, pp. 1297–1309, 2018, doi: 10.1016/j.applthermaleng.2017.09.086.

[14] C. Zotică, D. Pérez-Piñeiro, and S. Skogestad, "Supervisory control design for balancing supply and demand in a district heating system with thermal energy storage," *Comput. Chem. Eng.*, vol. 149, p. 107306, 2021, doi: 10.1016/j.compchemeng.2021.107306.

[15] J. Czeczot, P. Laszczyk, and M. Metzger, "Local balance-based adaptive control in the heat distribution system – practical validation," *Appl. Therm. Eng.*, vol. 30, no. 8, pp. 879–891, 2010, doi: 10.1016/j.applthermaleng.2009.12.021.

[16] J. Oravec, M. Bakošová, M. Trafczynski, A. Vasičkaninová, A. Mészáros, and M. Markowski, "Robust model predictive control and PID control of shell-and-tube heat exchangers," *Energy*, vol. 159, pp. 1–10, 2018, doi: 10.1016/j.energy.2018.06.106.

[17] H. Sano, "Finite-dimensional H_∞ control of a parallel-flow heat exchange process," *Bull. Pol. Acad. Sci. Tech. Sci.*, vol. 65, no. 1, pp. 11–19, 2017, doi: 10.1515/bpasts-2017-0002.

[18] R. Dyrska, M. Horváthová, P. Bakaráč, M. Mönnigmann, and J. Oravec, "Heat exchanger control using model predictive control with constraint removal," *Appl. Therm. Eng.*, vol. 227, p. 120366, 2023, doi: 10.1016/j.applthermaleng.2023.120366.

[19] X. Han, R. Rammal, M. He, Z. Li, M. Cabassud, and B. Dahhou, "Dynamic and sensor fault tolerant control for an intensified heat-exchanger/reactor," *Eur. J. Control*, vol. 69, p. 100736, 2023, doi: 10.1016/j.ejcon.2022.100736.

[20] Edibon, "Heat exchangers," https://www.edibon.com, accessed: November 28, 2025.

[21] Inteco, "Home page," https://www.inteco.com.pl, accessed: December 4, 2025.

[22] MathWorks, "Simulink desktop real-time — product page," https://www.mathworks.com/products/simulink-desktop-real-time.html, accessed: December 4, 2025.

[23] D. Pugliesi, "Functional levels of a distributed control system," https://commons.wikimedia.org/wiki/, 2014, cC BY-SA 3.0. Adapted version.

[24] B. Roffel and B.H. Betlem, *Advanced Practical Process Control*, 1st ed. Springer Berlin / Heidelberg, 2004, doi: 10.1007/978-3-642-18258-7.

[25] J. Li *et al.*, "Control method of multi-energy system based on layered control architecture," *Energy Build.*, vol. 261, p. 111963, 2022, doi: 10.1016/j.enbuild.2022.111963.

[26] C. Anuntasethakul and D. Banjerdpongchai, "Design of supervisory model predictive control for building HVAC system with consideration of peak-load shaving and thermal comfort," *IEEE Access*, vol. 9, pp. 41 066–41 081, 2021.

[27] C.J. Calfa, Z. O'Neill, Z. Yang, J. Wen, V. Adetola, and X. Liu, "Advances in supervisory control strategies for a heat pump centric HVAC system – a comprehensive review on applications," *Appl. Therm. Eng.*, vol. 279, p. 128059, 2025, doi: 10.1016/j.applthermaleng.2025.128059.

[28] A.M. Tayeb, M.A. El-Rifai, Y.A. El-Tawil, and R.M. Abdel-Monem, "Calculation of optimal controller settings and transient responses of a shell-and-tube heat exchanger," *Energy Convers. Manage.*, vol. 32, no. 5, pp. 431–438, 1991, doi: 10.1016/0196-8904(91)90004-3.

[29] M. Trafczynski, M. Markowski, S. Alabrudzinski, and K. Urbaniec, "Tuning parameters of PID controllers for the operation of heat exchangers under fouling conditions," *Chem. Eng. Trans.*, vol. 52, pp. 1237–1242, August 2016, doi: 10.3303/CET1652207.

[30] S. Ahmed, B. Huang, and S.L. Shah, "Novel identification method from step response," *Control Eng. Pract.*, vol. 15, no. 5, pp. 545–556, 2007, doi: 10.1016/j.conengprac.2006.10.005.

[31] G.A. Ramos and R. Costa-Castelló, "Optimal anti-windup synthesis for repetitive controllers," *J. Process Control*, vol. 23, no. 8, pp. 1149–1158, 2013, doi: 10.1016/j.jprocont.2013. 07.004.

[32] D. Horla, "Static anti-windup compensator based on BMI optimisation for discrete-time systems with directional change in controls avoidance," *Bull. Pol. Acad. Sci. Tech. Sci.*, vol. 72, no. 5, p. e151046, 2024.

[33] S.J. Rubavathy, B. Durai Babu, K. Sasikala, and S. Gomathi, "A comparative study of AVC-PDM and AVC-PWM based cyclo-inverter fed induction heating systems," *Res. Eng.*, vol. 25, p. 104402, 2025, doi: 10.1016/j.rineng.2025.104402.

[34] K.J. Åström and T. Hägglund, *Advanced PID Control*. Research Triangle Park, NC: ISA – The Instrumentation, Systems, and Automation Society, 2006.

[35] L. Estel, F. Bagui, M. Abdelghani-Idrissi, and C. Thenard, "Distributed state estimation of a counter current heat exchanger under varying flow rate," *Comput. Chem. Eng.*, vol. 24, no. 1, pp. 53–60, 2000, doi: 10.1016/S0098-1354(00)00301-X.

[36] K. Bartecki, “Steady-state analysis for a class of hyperbolic systems with boundary inputs,” *Arch. Control Sci.*, vol. 23, no. 3, pp. 295–310, 2013, doi: 10.2478/acsc-2013-0018.

[37] S. Qin and T.A. Badgwell, “A survey of industrial model predictive control technology,” *Control Eng. Pract.*, vol. 11, no. 7, pp. 733–764, 2003, doi: 10.1016/S0967-0661(02)00186-7.

[38] K. Bartecki, “Approximation of a class of distributed parameter systems using proper orthogonal decomposition,” in *16th IEEE International Conference on Methods and Models in Automation and Robotics*, Międzyzdroje, Poland, August 2011, pp. 351–356, doi: 10.1109/MMAR.2011.6031372.

[39] K. Bartecki, “PCA-based approximation of a class of distributed parameter systems: classical vs. neural network approach,” *Bull. Pol. Acad. Sci. Tech. Sci.*, vol. 60, no. 3, pp. 651–660, 2012.

[40] P.D. Christofides and P. Daoutidis, “Distributed output feedback control of two-time-scale hyperbolic PDE systems,” *Appl. Math. Comput. Sci.*, vol. 8, no. 4, pp. 713–732, 1998.

[41] T. Meurer, *Control of Higher–Dimensional PDEs: Flatness and Backstepping Designs*, 1st ed., ser. Communications and Control Engineering. Berlin Heidelberg: Springer-Verlag, 2012, doi: 10.1007/978-3-642-30015-8.